Journal of Alloys and Compounds 601 (2014) 100–103

Contents lists available at ScienceDirect

Journal of Alloys and Compounds

journal homepage: www.elsevier.com/locate/jalcom

Resistive switching and Schottky diode-like behaviors in $Pt/BiFeO_3/ITO$ devices

J.M. Luo [a,b,*], S.H. Chen [a], S.L. Bu [a], J.P. Wen [a]

[a] School of Physics and Optical Information Sciences, Jiaying University, Meizhou 514015, Guangdong, China
[b] State Key Laboratory of Optoelectronic Materials and Technologies, Sun Yat-Sen University, Guangzhou 510275, China

ARTICLE INFO

Article history:
Received 5 February 2014
Received in revised form 26 February 2014
Accepted 27 February 2014
Available online 12 March 2014

Keywords:
Bismuth ferrite
Resistive switching
Schottky effect
Conductive filament

ABSTRACT

$Pt/BiFeO_3/ITO$ devices with nonvolatile bipolar resistive switching characteristic have been fabricated by chemical solution deposition. When applying the positive bias on Pt top electrodes, both bipolar and unipolar resistive switching can be observed after a forming process; however, when applying the negative bias, no forming and resistive switching but a rectifying diode-like effect can be found. This behavior has been analyzed by current conduction in detail, and then can be understood in terms of conductive filament mechanism with considering Schottky effect at $BiFeO_3/ITO$ interface.

1. Introduction

Resistive random access memory (RRAM), based on resistive switching (RS) effect, is considered as one of the most competitive candidates for next-generation nonvolatile memories. On account of this promise, a variety of resistance-switch materials have been extensively investigated in theories and experiments [1–4]. In recent years, multiferroic bismuth ferrite (BFO) has also been reported to show the superior RS characteristics [5–8], receiving widespread interest for its fascinating potential in the novel multifunctional devices.

For the development of BFO applications in practical devices, the physical origin of RS should be addressed and solved. Two basic models are usually proposed to explicate the RS behaviors of BFO-based thin films, including filamentary-type model [9] where the resistance switching originates from the formation and rupture of conductive filament in the thin film, and interface-type model [10] where the resistance switching takes place at the interface between the electrode and the thin film. Luo et al. [6] reported the nonpolar resistive switching in Mn-doped BFO thin films deposited on $Pt/Ti/SiO_2/Si$ substrates, which is attributed to the valence change between Fe^{3+} and Fe^{2+} due to the neutralization and ionization of oxygen vacancies (OVs); Chen et al. [7] explained the RS property of BFO thin films on $LaNiO_3$-buffered Si substrates by the modification of Schottky-like barrier due to the drift of OVs; Shuai et al. [8] found the interface-related RS behavior in BFO thin films grown on $Pt/Ti/SiO_2/Si$ substrates but no observation on Pt/sapphire substrates. From these studies, substrate effect is considered to play an important role on the RS behaviors. Recently, BFO thin films grown on ITO/glass substrates were reported to show advantageous electrical and ferroelectric characteristics, which can be useful in nonvolatile resistance memory devices or tunable diodes [11]. In this work, nonvolatile resistive switching has been investigated in Pt/BFO/ITO structures. When initially applying the positive bias on Pt top electrodes, both bipolar resistive switching (BRS) and unipolar resistive switching (URS) can be observed after a forming process; however, no forming and resistive switching but a Schottky effect can be found with the negative bias. This behavior has been discussed in detail.

2. Experimental

BFO thin films were deposited on ITO/glass substrates by the sol–gel method. $Bi(NO_3)_3{\cdot}5H_2O$ and $Fe(NO_3)_3{\cdot}9H_2O$ were used to prepare the precursor solution. The BFO solution was spin-coated and dried for several times under the same conditions, and then annealed in air at 600 °C for 30 min. The structure of films was analyzed by X-ray diffraction (XRD, D-MAX 2200VPC), the cross-section morphology was examined with scanning electron microscopy (SEM, Quanta 400F), and the surface morphology was characterized using a scanning probe microscope (SPM, CSPM5500). After Pt top electrodes deposited on the films with a diameter of 0.3 mm, the current–voltage curves were measured by a semiconductor characterization system (SCS, Keithley 4200).

* Corresponding author at: School of Physics and Optical Information Sciences, Jiaying University, Meizhou 514015, Guangdong, China. Tel.: +86 0753 2186808; fax: +86 0753 2354179.
E-mail address: zsuljm@163.com (J.M. Luo).

http://dx.doi.org/10.1016/j.jallcom.2014.02.180
0925-8388/

3. Results and discussion

Fig. 1(a) shows the XRD patterns for BFO thin film deposited on ITO/glass substrate. All of the diffraction peaks indicate the distorted rhombohedral perovskite crystal structure of BFO, and no impurity phase can be observed. The cross-section morphology of thin film is demonstrated in the inset of Fig. 1(a), suggesting that the thin film is well-grown on ITO/glass substrate with thickness of about 300 nm. Fig. 1(b) shows the SPM measurement performed in the region of 1.2 × 1.2 μm^2, and a large crystalline grain can be observed in the BFO polycrystalline film.

Fig. 2 exhibits the typical leakage current property of BFO thin film with the bottom electrode ITO grounded and the top electrode Pt applied to a sweeping voltage of −5 V—0 V—5 V. This structure shows a diode-like behavior with a rectification ratio of about 8 at ±5 V, which is supposed to be originating from the Schottky contact at the interface of BFO thin film and ITO substrate.

The nonvolatile BRS characteristic of Pt/BFO/ITO memory devices has been demonstrated in Fig. 3(a), where the arrows represent the direction of sweeping voltage. To activate the memory device, a forming process is necessary by applying a high positive voltage and a compliance current (CC) on Pt electrode, which is shown in the inset of Fig. 3(a). After that, the current–voltage properties of BRS have been measured for 100 switching cycles. When the positive voltage increases, the current rapidly increases at a "set" voltage (V_{set}), and the device switches from high resistive state (HRS) to low resistive state (LRS). When a negative "reset" voltage (V_{reset}) is applied, the current suddenly drops to a low value, and the device switches back to HRS. The switching parameters (V_{set} and V_{reset}) with switching cycles have been plotted in Fig. 3(b). During a continuously automatic dc sweeping bias, Pt/BFO/ITO memory devices could switch to LRS or HRS with low-voltage dispersion during the 100 switching cycles. Moreover, the resistance evolution of HRS and LRS has also been demon-

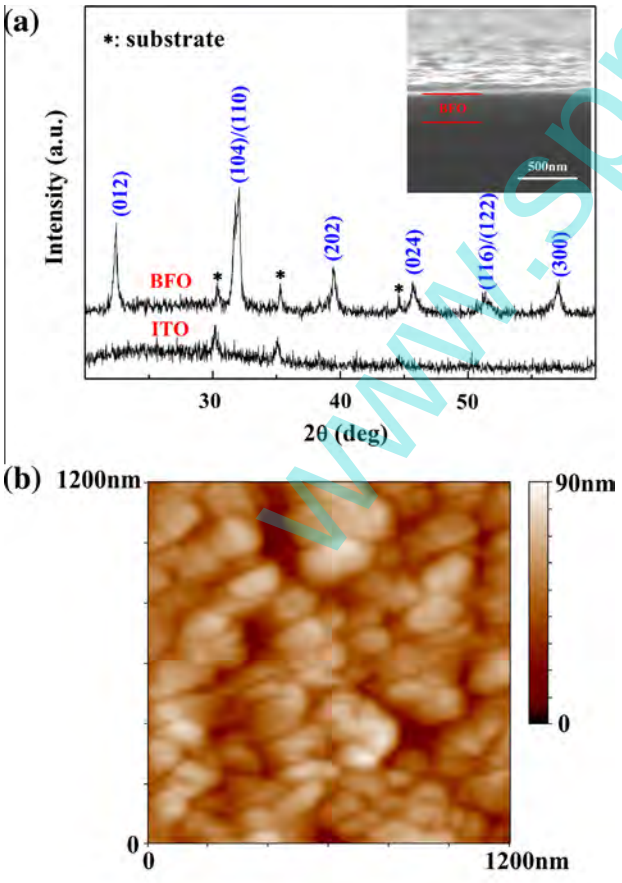

Fig. 1. (a) XRD patterns and (b) SPM image of BFO thin film. The inset of (a) shows the cross-section morphology.

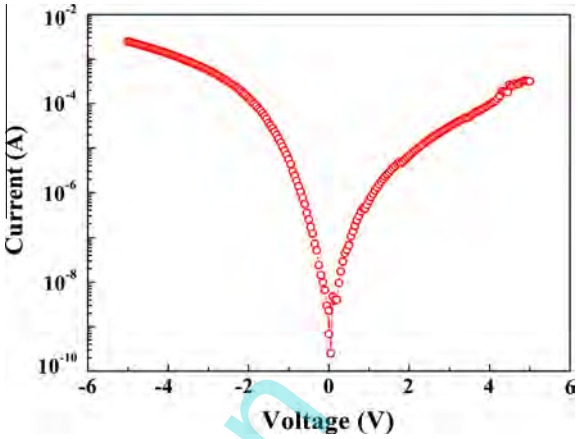

Fig. 2. Rectifying leakage current in Pt/BFO/ITO devices.

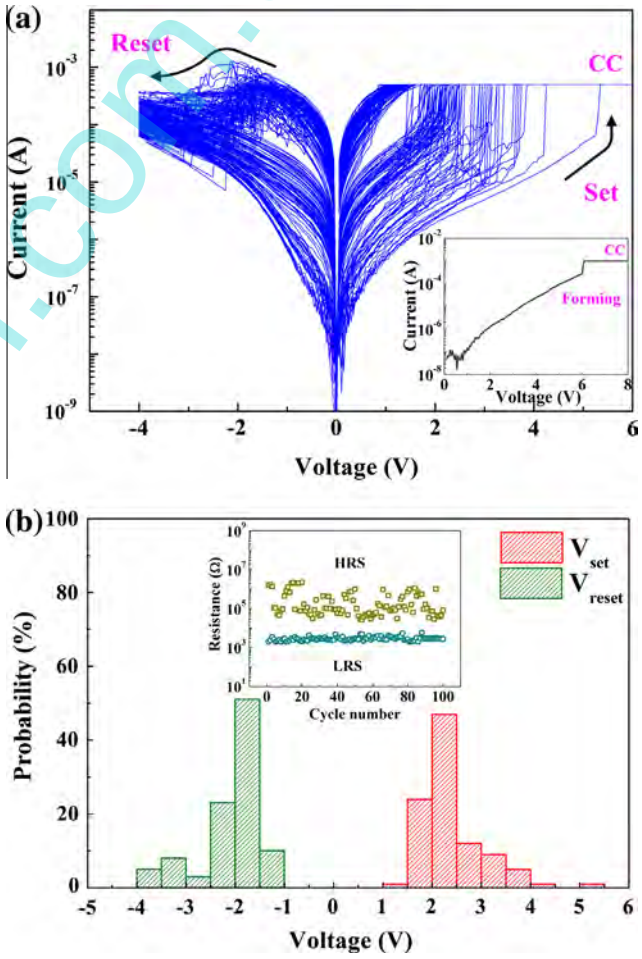

Fig. 3. BRS characteristics in Pt/BFO/ITO devices. (a) Current–voltage curves with 100 cycles, sweeping step = 0.05 V, delay time = 50 ms and CC = 0.5 mA. The inset shows the forming process. (b) Distribution of set and reset voltages. The inset demonstrates the resistance evolution of HRS and LRS with switching cycles at a read voltage of 1 V.

strated in the inset of Fig. 3(b). The resistance ratio is about one order of magnitude, and the resistance in HRS shows large-resistance dispersion. According to filamentary-type model, the formation and rupture of conductive filament could be random and localized, which is determined by the migration of OVs, depending on the non-uniform distribution of electric field, OV concentration and temperature. This can be the reason for the fluctuation of switching voltages and resistance.

In the preceding measurements, as illustrated in Fig. 4(a), both BRS and URS can be clearly observed after the initial forming process by applying the positive voltage on Pt electrode. However, when applying the negative voltage on the device in HRS, no forming and RS can be found until −20 V. This RS behavior with diode-like property is different from the RS characteristic observed in the symmetrical structures of memory devices [7,12]. To further understand the physical origin of this behavior, the study of conduction mechanisms is required. For the positive voltage range in Fig. 4(b), when the majority of electron traps (e.g. OVs) are emptied, the current–voltage characteristic is dominated by the traps. In this case, the current–voltage curve in HRS fits well by the trap-limited space-charge-limited current (TL-SCLC) conduction with an exponentially distributed trap [13]:

$$J = N_c \mu e \left(\frac{\varepsilon_r \varepsilon_0}{eN_t}\right)^l \left(\frac{l}{l+1}\right)^l \left(\frac{2l+1}{l+1}\right)^{l+1} \frac{V^{l+1}}{L^{2l+1}} \quad (1)$$

where N_c is the electron density of states, N_t is the total trap states per unit volume, μ is the field independent mobility, e is the charge of electrons, ε_r is the related dielectric constant, ε_0 is the permittivity of free space, L is the thickness of films, and l is defined as the ratio of the characteristic temperature of the trap distribution to the operating temperature. From Fig. 4(b), in the low positive voltage range of HRS ($V < V_0$), the current–voltage behavior obeys the Ohmic law (slope: $l + 1 \sim 1$). Whereas in the high positive voltage range of HRS ($V > V_0$), the current conduction follows the TL-SCLC mechanism (slope: $l + 1 > 1$). When the majority of electron traps are occupied with the injected electrons and connected to form a filamentary conducting path, the current behavior shows an Ohmic conduction property in LRS. However, for the negative voltage range, the current conduction in HRS seems different. As shown in Fig. 4(c), in the low negative voltage range ($0 < V < V_2$), the conduction mechanism is similar to that in the positive voltage range. While in the high negative voltage range ($V_2 < V < V_3$), the slope is about 2, indicating the Child's law can be attained by filling the entire trap sites with the injected electrons. When applying the higher negative voltage above V_3, the slope is nearly 1, indicative of a quasi-Ohmic property. This behavior cannot be understood by the SCLC model. Considering the rectifying diode-like effect, the current–voltage characteristic of HRS in the negative voltage range has also been analyzed using the Schottky emission model [13]:

$$J_s = AT^2 \exp\left(-\frac{e\phi - \sqrt{e^3 V / 4\pi K \varepsilon_0 L}}{k_B T}\right) \quad (2)$$

where A is the Richardson constant, h is the Planck constant, $e\phi$ is the Schottky barrier height, K is the optical dielectric permittivity, T is temperature. The refraction index for BFO is known to be $n = 2.5$, and thus the optical dielectric permittivity of $K = n^2 = 6.25$ is expected [14]. From the fitting result of Fig. 4(d), the optical dielectric permittivity K can be derived to be 6.62 in the high negative voltage range ($V_2 < V < V_3$), which is in good agreement with the ideal optical dielectric permittivity. Therefore, it is reasonable to believe that the current in this voltage range could be greatly contributed by the Schottky emission.

In general, filamentary-type model without considering Schottky effect can be applied to interpret both BRS and URS behaviors, whereas interface-type model is used for BRS but difficult for URS. Accordingly, based on the aforementioned analysis, a conductive filament mechanism with considering the Schottky effect at the BFO/ITO interface has been proposed, the sketches of

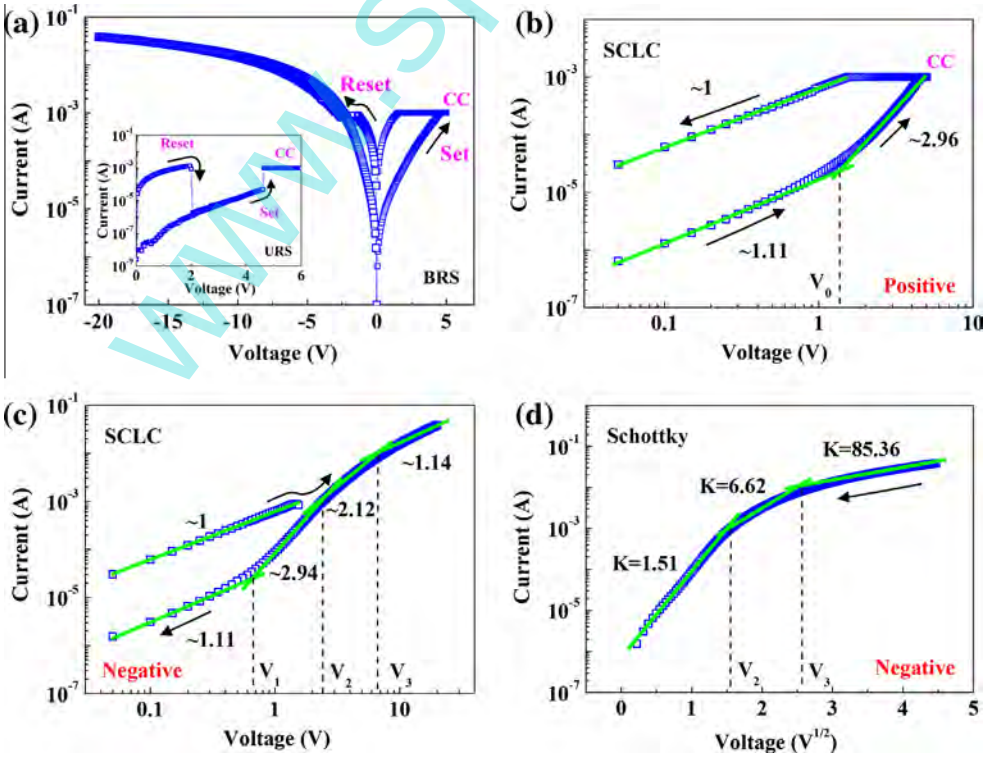

Fig. 4. Resistive switching and diode-like behaviors in Pt/BFO/ITO devices. (a) Typical current–voltage property of BRS. The inset shows the current–voltage property of URS. Data fitting of current conduction: (b) SCLC at the positive voltage range; (c) SCLC and (d) Schottky emission at the negative voltage range.

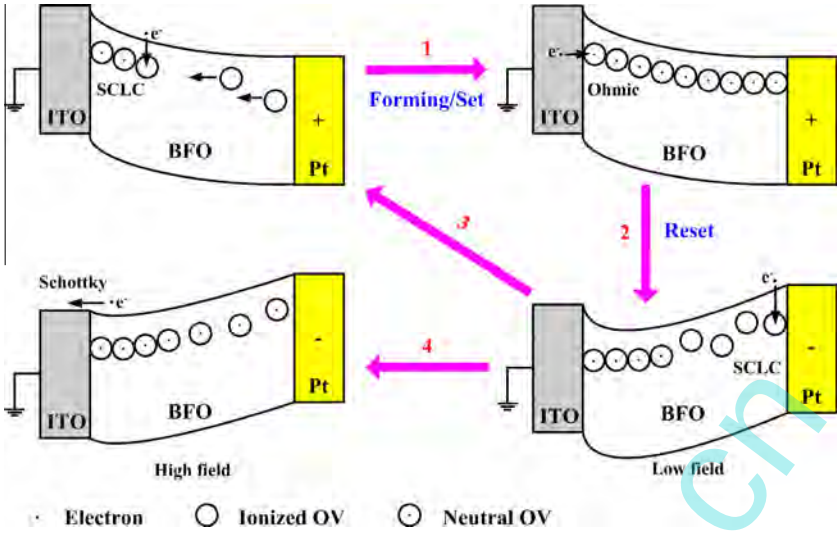

Fig. 5. Sketches of the conductive filament mechanism with considering the Schottky effect.

which are depicted in Fig. 5. When applying the positive voltage on the Pt electrode, due to the Schottky effect of the BFO/ITO interface, most of electrons are blocked at the ITO electrode, such that few electrons can be injected into the BFO thin film, leading to the SCLC conduction. On the other hand, the ionized OVs can migrate and capture the injected electrons to become neutral, and then these neutralized OVs are connecting and forming a conductive filament, which is known as "forming/set" (Process 1). Once the filament is formed, the rupture of filament can be achieved by applying either positive bias (URS) or negative bias (BRS), which is known as "reset" (Process 2). These set-reset processes can be reproduced with cycles (Process 3), just as observed in Fig. 3. However, when applying the high negative voltage on the Pt electrode, the Schottky barrier height at the BFO/ITO interface can be significantly lowered, leading to the Schottky emission from the thin film to the ITO electrode, and as a result the ionized OVs can be easily occupied with the injected electrons, forcing the neutralized OVs disconnecting and difficult to form a conductive filament (Process 4), which could be the reason for the disappearance of "forming/set" process with the negative bias. When the negative voltage is higher enough, the Schottky barrier height gets further lower, and then the Schottky contact could convert into the quasi-Ohmic contact.

4. Conclusions

In summary, Pt/BFO/ITO memory devices show the nonvolatile resistive switching characteristic. Both bipolar and unipolar resistive switching can be measured after the forming process by applying the high positive bias on Pt electrode; while no forming and resistive switching but the Schottky diode-like effect can be observed with the negative bias. According to the analysis of current conduction, this asymmetric behavior can be interpreted by the conductive filament mechanism with considering the Schottky effect at the BFO/ITO interface, indicating that a multifunctional device application would be feasible.

Acknowledgements

The authors greatly acknowledge Prof. B. Wang and Prof. Y. Zheng (Sun Yat-Sen University) for valuable suggestions and Dr. S.P. Lin for helpful discussions. The authors also thank the financial support from the Natural Science Foundation of Guangdong Province (No. S2012010010976).

References

[1] D.S. Jeong, R. Thomas, R.S. Katiyar, J.F. Scott, H. Kohlstedt, A. Petraru, C.S. Hwang, Prog. Phys. 75 (2012) 076502.
[2] M. Pilch, A. Molak, J. Alloys Comp. 586 (2014) 488–498.
[3] J.M. Luo, R.Q. Chen, S.P. Lin, Phys. Status Solidi A 211 (2014) 191–194.
[4] J.M. Luo, Int. J. Mod. Phys. B 27 (2013) 1350160.
[5] C.H. Yang, J. Seidel, S.Y. Kim, P.B. Rossen, P. Yu, M. Gajek, Y.H. Chu, L.W. Martin, M.B. Holcomb, Q. He, P. Maksymovych, N. Balke, S.V. Kalinin, A.P. Baddorf, S.R. Basu, M.L. Scullin, R. Ramesh, Nat. Mater. 8 (2009) 485–493.
[6] J.M. Luo, S.P. Lin, Y. Zheng, B. Wang, Appl. Phys. Lett. 101 (2012) 062902.
[7] X. Chen, H. Zhang, K. Ruan, W. Shi, J. Alloys Comp. 529 (2012) 108–112.
[8] Y. Shuai, X. Qu, C. Wu, W. Zhang, S. Zhou, D. Burger, H. Reuther, S. Slesazeck, T. Mikolajick, M. Helm, J. Appl. Phys. 111 (2012) 07D906.
[9] R. Waser, M. Aono, Nat. Mater. 6 (2007) 833–840.
[10] A. Sawa, Mater. Today 11 (2008) 28–36.
[11] Y. Yao, B. Zhang, L. Chen, Y. Yang, Z. Wang, H.N. Alshareef, X.X. Zhang, J. Phys. D: Appl. Phys. 46 (2013) 055304.
[12] H.H. Huang, W.C. Shih, C.H. Lai, Appl. Phys. Lett. 96 (2010) 193505.
[13] C. Hamann, H. Burghardt, T. Frauenheim, Electrical Conduction Mechanisms in Solids, VEB Deutscher Verlag der Wissenschaften, Berlin, 1988.
[14] S. Iakovlev, C.H. Solterbeck, M. Kuhnke, M. Es-Souni, J. Appl. Phys. 97 (2005) 094901.